



UNIVERSITY OF LEEDS

This is a repository copy of *Successive elimination of shear layers by a hierarchy of constraints in inviscid spherical-shell flows*.

White Rose Research Online URL for this paper:
<http://eprints.whiterose.ac.uk/76564/>

Version: Published Version

Article:

Livermore, PW and Hollerbach, R (2012) Successive elimination of shear layers by a hierarchy of constraints in inviscid spherical-shell flows. *Journal of Mathematical Physics*, 53 (7). 073104. ISSN 0022-2488

<https://doi.org/10.1063/1.4736990>

Reuse

Unless indicated otherwise, fulltext items are protected by copyright with all rights reserved. The copyright exception in section 29 of the Copyright, Designs and Patents Act 1988 allows the making of a single copy solely for the purpose of non-commercial research or private study within the limits of fair dealing. The publisher or other rights-holder may allow further reproduction and re-use of this version - refer to the White Rose Research Online record for this item. Where records identify the publisher as the copyright holder, users can verify any specific terms of use on the publisher's website.

Takedown

If you consider content in White Rose Research Online to be in breach of UK law, please notify us by emailing eprints@whiterose.ac.uk including the URL of the record and the reason for the withdrawal request.



eprints@whiterose.ac.uk
<https://eprints.whiterose.ac.uk/>

Successive elimination of shear layers by a hierarchy of constraints in inviscid spherical-shell flows

Philip W. Livermore and Rainer Hollerbach

Citation: *J. Math. Phys.* **53**, 073104 (2012); doi: 10.1063/1.4736990

View online: <http://dx.doi.org/10.1063/1.4736990>

View Table of Contents: <http://jmp.aip.org/resource/1/JMAPAQ/v53/i7>

Published by the AIP Publishing LLC.

Additional information on J. Math. Phys.

Journal Homepage: <http://jmp.aip.org/>

Journal Information: http://jmp.aip.org/about/about_the_journal

Top downloads: http://jmp.aip.org/features/most_downloaded

Information for Authors: <http://jmp.aip.org/authors>

ADVERTISEMENT

physicstoday

Comment on any
Physics Today article.

Physics Today | Volume 63 | 14 July 2012
Previous Article | Next Article

Measured energy in Japan
David von Seggern
(dovseg@seismo.unr.edu) University of Nevada
July 2012, page 10
DIGITAL OBJECT IDENTIFIER
<http://dx.doi.org/10.1063/PT.3.1619>

The article by Thorne Lay and Hiroo Kanamori (PT.3.1619) is an excellent review of the seismic energy release from the 11-March 2011 earthquake in Japan. The authors' estimate of the seismic energy release is approximately five times as much energy as the 100-megaton atomic bomb that was dropped on Nagasaki in August 1945. The authors' estimate is based on the seismic energy release from the earthquake, which is a measure of the energy released by the rupture of the fault. The authors' estimate is based on the seismic energy release from the earthquake, which is a measure of the energy released by the rupture of the fault. The authors' estimate is based on the seismic energy release from the earthquake, which is a measure of the energy released by the rupture of the fault.

Comment on this article
By the act of hitting a ball with a bat, one calculates the force energy to deliver the ball to its new location, but one must also take into account that the ball extended its energy to the entire team, which became struck by the ball as its momentum ceased and passed energy to the entire team. Therefore the parameters of the damage extend into the future when the received energy to that pushed upon, later becomes released in a new event. Perhaps calculations of one added that in, while another's calculations did not. E.M.C.
Written by Edgar Mocarvill, 14 July 2012 19:59

Successive elimination of shear layers by a hierarchy of constraints in inviscid spherical-shell flows

Philip W. Livermore¹ and Rainer Hollerbach^{2,3}

¹*School of Earth & Environment, University of Leeds, Leeds LS2 9JT, United Kingdom*

²*School of Mathematics, University of Leeds, Leeds LS2 9JT, United Kingdom*

³*Institut für Geophysik, ETH Zürich, 8092 Zürich, Switzerland*

(Received 22 August 2011; accepted 26 June 2012; published online 26 July 2012)

In a rotating spherical shell, an inviscid inertia-free flow driven by an arbitrary body force will have cylindrical components that are either discontinuous across, or singular on, the tangent cylinder, the cylinder tangent to the inner core and parallel to the rotation axis. We investigate this problem analytically, and show that there is an infinite hierarchy of constraints on this body force which, if satisfied, sequentially remove discontinuities or singularities in flow derivatives of progressively higher order. By splitting the solution into its equatorial symmetry classes, we are able to provide analytic expressions for the constraints and demonstrate certain inter-relations between them. We show numerically that viscosity smoothes any singularity in the azimuthal flow component into a shear layer, comprising inner and outer layers, either side of the tangent cylinder, of width $O(E^{2/7})$ and $O(E^{1/4})$, respectively, where E is the Ekman number. The shear appears to scale as $O(E^{-1/3})$ in the equatorially symmetric case, although in a more complex fashion when considering equatorial antisymmetry, and attains a maximum value in either the inner or outer sublayers depending on equatorial symmetry. In the low-viscosity magnetohydrodynamic system of the Earth's core, magnetic tension within the fluid resists discontinuities in the flow and may dynamically adjust the body force in order that a moderate number of the constraints are satisfied. We speculate that it is violations of these constraints that excites torsional oscillations, magnetohydrodynamic waves that are observed to emanate from the tangent cylinder. © 2012 American Institute of Physics. [<http://dx.doi.org/10.1063/1.4736990>]

I. INTRODUCTION

The study of shear layers in hydrodynamic flows has a long history. In a rotating, spherical-shell geometry, analytic progress dates back to the seminal work of Proudman¹⁸ and Stewartson²² in which they considered a low-viscosity system which was driven through a small relative difference, $\epsilon \ll 1$, in the angular velocity of the boundary surfaces. The primary flow driven by the motion of the boundaries is that of a simple solid body rotation, although of considerably more interest is the secondary flow of magnitude $O(\epsilon)$ which is induced by viscous stresses at the boundaries. This flow is axisymmetric and, due to the strong influence of rotation, essentially geostrophic (i.e., azimuthal and independent of the axial coordinate) except in the vicinity of certain boundary layers. Of paramount importance is the internal boundary layer on the tangent cylinder (denoted \mathcal{C}), the axial cylinder tangent to the inner sphere, which divides the spherical shell into two subdomains. Outside \mathcal{C} the geostrophic cylinders (axial cylinders on which the flow is constant) intersect only the outer boundary and the flow rotates as a solid body, oblivious to the differential boundary rotation of the inner sphere. Inside \mathcal{C} each geostrophic cylinder intersects both spherical boundaries and a formal asymptotic treatment for small viscosity at fixed ϵ shows that the geostrophic velocity is nonzero and intermediate between that of the outer and inner spherical boundaries, attaining that of the inner sphere on the inner-side of \mathcal{C} . Thus across \mathcal{C} the azimuthal component of the flow is

formally discontinuous in the inviscid limit. However, by reinstating a weak viscosity, the solution is rendered continuous by a nested sequence of free-shear (so-called Stewartson) layers.

One important application of these ideas is to the Earth's liquid core, for which there is evidence that the solid inner core may rotate at a different rate to the exterior mantle.²⁰ So-called spherical Couette flows as described above, along with their associated shear layers, may therefore play a role in the dynamics of the Earth's core. However, more detailed studies bound the differential rotation by about $0.2^\circ/\text{year}$, in many cases within an error tolerance of zero.²³ Even if nonzero, such a super-rotation of the inner core is very small when compared with the daily rotation of the planet, corresponding to a value of $\epsilon = O(10^{-6})$. Due to their small magnitude, such shear layers driven by this process would not likely be of significant dynamical importance.

Motivated by the strong magnetic field in Earth's core, we consider instead a flow \mathbf{u} , driven not by boundary effects but by an internal body force.¹⁰ The body force \mathbf{f} comprises not only the Lorentz force due to the magnetic field, but also buoyancy which ultimately powers the geodynamo^{3,13} (for recent reviews). Both direct observations and geodynamo models indicate that the magnitude of the body force \mathbf{f} (for instance, as measured by the Elsasser number) is comparable to that of rotational (Coriolis) forces⁵ and, being of $O(1)$ rather than $O(\epsilon)$, can drive strong flows and associated dynamically important shear layers. The focus of this paper is to address what properties of \mathbf{f} lead to the formation of shear layers; or, expressed in another way, if the system dynamically favours a smooth flow, the manner in which \mathbf{f} must change in order to avoid discontinuities.

Although similar in many respects, the boundary-driven case has some significant differences from the internally forced system. From a mathematical point of view, of fundamental importance is that inviscid solutions may be written down directly in the latter case. In the boundary-driven system, the geostrophic flow is unspecified by the inviscid equations and is determined only by the low-viscosity limit of an involved viscous boundary-layer solution. Furthermore, since the forced flow depends everywhere on (the spatially dependent) \mathbf{f} , it too may be dependent on the axial coordinate rather than simply geostrophic. However, in both cases the flow depends on the boundary conditions which, due to rotation, are only communicated parallel to the rotation axis (when ignoring viscosity). Thus, even in the forced system, only inside \mathcal{C} does the inner core have any influence and, in general, on \mathcal{C} any inviscid solution will have components that are each either discontinuous or singular; indeed, by restricting the possible choices of \mathbf{f} to a subclass which satisfies a certain homogeneous constraint, it is possible to render continuous the cylindrically radial component of flow, u_s , on \mathcal{C} , following the work of Hollerbach and Proctor.¹⁰ This may be viewed as encoding into \mathbf{f} the existence of the inner core, making the solution outside \mathcal{C} "aware" of the matching condition that it should satisfy. However, this constraint guarantees continuity only of u_s ; other components, for instance, u_ϕ (the azimuthal component of flow) may be not only discontinuous but singular on \mathcal{C} .

The purpose of this paper is to investigate, analytically, the structure of an inviscid, inertia-free fluid subject to a body force \mathbf{f} , and to determine the constraints on \mathbf{f} that are both necessary and sufficient in order to ensure any given continuity condition on the (non-axisymmetric) flow. Indeed, we will show that there is a hierarchy of such conditions, of which the Hollerbach-Proctor constraint is the first, which progressively smooth the flow on \mathcal{C} . If a sufficient number of these conditions are satisfied then the inviscid flow will be smooth enough on \mathcal{C} that, if the weakly viscous problem were to be considered, any Stewartson-like shear layers would be entirely eliminated. As may be anticipated, this ordered list of constraints progressively include information about ever higher order derivatives of the body force and become inherently more mathematically complex statements. For instance, although the Hollerbach-Proctor constraint involves only a certain simple average of $\nabla \times \mathbf{f}$ over \mathcal{C} , subsequent constraints involve a mixture of much more complex averages combined with pointwise values of \mathbf{f} . Although we provide a general methodology to produce constraints to arbitrary order, in view of the complexity and typographic limitations, we provide only the first five members of the constraint hierarchy, these being sufficient to ensure that not only the flow but all of its first order derivatives are continuous on \mathcal{C} . It is worth remarking that, even if the constraints are not satisfied, the (possibly only piecewise continuous) solution for the non-axisymmetric flow can always be found. This is quite different from the axisymmetric case in which there is no solution unless Taylor's constraint²⁴ is satisfied. Even if it is, the geostrophic flow is arbitrary and requires a further equation to close the system.

In the MHD system, the resistance to shear of magnetic field lines embedded in the fluid has a significant impact on the dynamics. In the Stewartson boundary-driven case, several studies have shown that the Lorentz force, associated with induced magnetic fields in the vicinity of strong velocity gradients, act to suppress the tangent-cylinder shear layers.^{4,8,12} In systems driven by a body force, similar adjustments occur and indeed there is numerical evidence⁷ that the magnetic field arranges itself to satisfy the Hollerbach-Proctor constraint, required for continuity of u_s on \mathcal{C} . In order for the magnetic field to have such a pronounced effect, not only must it be sufficiently strong, i.e., comparable to the Coriolis force, but it must be of the correct geometry. This latter qualification is important as field lines must cross \mathcal{C} , coupling the two regions together in order to eliminate discontinuities in the flow. In particular, owing only to symmetry, dipolar fields do not cross \mathcal{C} on the equator and are therefore inefficient at removing the boundary-layer stump attached to the inner sphere.²¹ In this study, we discount the possibility of dynamical adjustment and simply consider \mathbf{f} as prescribed.

The remainder of the paper is laid out as follows. In Sec. II, we describe the model setup and give a complete solution of the flow in the forced, inviscid, non-axisymmetric problem. In Sec. III we derive a hierarchy of constraints on \mathbf{f} that ensure continuity across \mathcal{C} of any given component of the flow, and also confirm that the solution is finite on the rotation axis. In Sec. IV we provide some analytic examples illustrating the key ideas, and in Sec. V we explore how the singularities and discontinuities that may arise are smoothed into shear layers of finite thickness by viscosity. We end with a discussion in Sec. VI.

II. A COMPLETE DESCRIPTION OF THE INVISCID FORCED FLOW

We consider the forced, nondimensional Navier-Stokes equations in a frame that rotates about the z axis:

$$2\mathbf{k} \times \mathbf{u} = -\nabla p + \mathbf{f} + \left[E \nabla^2 \mathbf{u} - R_o \frac{D\mathbf{u}}{Dt} \right], \quad (1)$$

where \mathbf{k} is the unit vector in the z -direction, \mathbf{u} is the incompressible velocity, p is the pressure, and \mathbf{f} is a body force. Owing to the magnitude of the Rossby number (measuring the ratio of inertial to rotational effects), $R_o = O(10^{-9})$, and the Ekman number (measuring the ratio of viscosity to rotational effects), $E = O(10^{-15})$, in the Earth's core,⁵ we neglect both viscosity and the inertial terms in the square parenthesis. In later sections, we will discuss how the system may be altered when these terms are added back in. In the specific application of the geodynamo, \mathbf{f} is simply the sum of the Lorentz and buoyancy forces, although for the present purposes it may be considered arbitrary but smooth (that is, it has continuous derivatives of all orders). We will solve (1) in a spherical-shell geometry which is most efficiently described in spherical polar coordinates (r, θ, ϕ) as the domain $r_i \leq r \leq r_o$, where r_i and r_o are the inner and outer boundary radii. However, owing to the importance of the tangent cylinder, cylindrical polar coordinates (s, ϕ, z) will also be used throughout. In our rotating frame, the physical system of interest is modelled by considering both (stationary) boundaries as impenetrable and nonslip. However, in the inviscid case, due to the removal of the highest derivative in (1), only impenetrable conditions may be employed and the flow may have nonzero slip on $r = r_i, r_o$. It is assumed that, on reinstating weak viscosity, the solution will be modified by thin Ekman layers on both spherical boundaries, which form only in order to bring the fluid to rest and do not influence the free-stream solution (this will be justified by example in Sec. IV). Note that this stands in stark contrast to the boundary-forced spherical Couette case in which the secondary flow is driven entirely by Ekman pumping.

In the inviscid inertia-free limit of interest, $R_o = E = 0$, an explicit solution (exploiting incompressibility) may be immediately written down by first taking the curl,

$$\frac{d\mathbf{u}}{dz} = -\mathbf{L}, \quad (2)$$

where $\mathbf{L} = \frac{1}{2} \nabla \times \mathbf{f}$ and then integrating with respect to z . In what follows, some of the ensuing algebraic expressions will be reduced in length by the introduction of the vector \mathbf{L} .

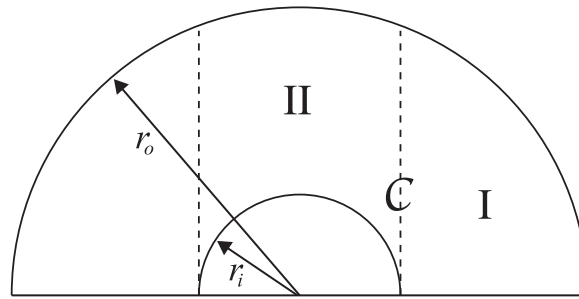


FIG. 1. Regions of the spherical-shell geometry restricted to the upper hemisphere; the tangent cylinder, \mathcal{C} , separates equatorial regions (I) from the polar regions (II).

Equation (2) is not only linear but in fact its solutions separate into symmetry classes depending on the equatorial symmetry of \mathbf{f} . Recall that a vector \mathbf{v} is equatorially symmetric (E^S) if both v_s and v_ϕ are even functions of z and v_z is odd; conversely, \mathbf{v} is equatorially antisymmetric (E^A) if both v_s and v_ϕ are odd and v_z is even in z . Further, it is elementary to show that (i) $\nabla \times \mathbf{v}$ is E^A (E^S) if and only if \mathbf{v} is E^S (E^A) and (ii) $d\mathbf{v}/dz$ is E^A (E^S) if and only if \mathbf{v} is E^S (E^A). It follows that \mathbf{u} is E^A (E^S) and \mathbf{L} is E^S (E^A) if \mathbf{f} is E^A (E^S). Therefore, rather than solving (2) in the entire spherical shell, it is expedient to solve for each symmetry separately, in each case restricting attention to the upper hemisphere. The geometry under consideration is shown in Figure 1.

At any cylindrical radius $0 \leq s \leq r_o$, let us define the vector \mathbf{I} as the following componentwise integral of \mathbf{L} :

$$I_{s,\phi,z}(s, \phi, z) = \int_z^{z_o} L_{s,\phi,z}(s, \phi, z') dz'$$

with $z_o = \sqrt{r_o^2 - s^2}$. The solution to (2) may then be written succinctly as

$$\mathbf{u} = [I_s, I_\phi, I_z](s, \phi, z) + [c_s, c_\phi, c_z](s, \phi), \quad (3)$$

where c_s, c_ϕ , and c_z are constants of the integration with respect to z , which depend on the remaining variables (s, ϕ) . Since z_o marks the top of the outer boundary in both regions I and II, \mathbf{I} is smooth everywhere in the upper hemisphere. Note that since \mathbf{c} is independent of z , the boundary conditions are communicated in the z -direction and so \mathbf{c} must be found in regions I and II separately. Thus, the solution in region I is oblivious to the inner core, leading to possible discontinuities on \mathcal{C} . Furthermore, due to the vertical slope of the inner boundary surface on \mathcal{C} , the solution in II may even admit singular behaviour.

In region II, in which $s \leq r_i$, the non-penetration condition $\mathbf{u} \cdot \mathbf{r} = \mathbf{u} \cdot [s, 0, z] = 0$, where \mathbf{r} is the position vector, at both $r = r_o$ and $r = r_i$ supply the conditions

$$s c_s + z_o c_z = 0, \quad (4)$$

$$s (I_s(z_i) + c_s) + z_i (I_z(z_i) + c_z) = 0, \quad (5)$$

where $z_i = \sqrt{r_i^2 - s^2}$ and has solution

$$c_s = \frac{z_o (s I_s(z_i) + z_i I_z(z_i))}{s(z_i - z_o)}, \quad c_z = -\frac{s I_s(z_i) + z_i I_z(z_i)}{(z_i - z_o)}, \quad (6)$$

where we suppress the dependence of \mathbf{I} on (s, ϕ) for typographic purposes. Note that c_s is everywhere finite in region II (even at $s = r_i$), except possibly at $s = 0$.

The solution in region I, in which $s > r_i$, is found slightly differently. Since it has no boundary on the equator, in addition to the non-penetration condition at $r = r_o$ we consider a symmetry condition on \mathbf{u} : if $\mathbf{u} \in E^S$ then $u_z = 0$ on the equator; conversely if $\mathbf{u} \in E^A$ then $u_s = 0$ on the equator. In region

I, the solution is then

$$c_s = \begin{cases} \frac{z_0}{s} \int_0^{z_0} L_z dz & \mathbf{u} \in E^S \\ - \int_0^{z_0} L_s dz & \mathbf{u} \in E^A \end{cases} \quad (7)$$

with $c_z = -s c_s / z_0$. The meridional flow is now completely specified in both regions; the remaining u_ϕ component is determined in the axially non-symmetric case by using the divergence-free property:

$$\frac{\partial u_\phi}{\partial \phi} = -\frac{\partial(s u_s)}{\partial s} - s \frac{\partial u_z}{\partial z} = -\frac{\partial(s c_s)}{\partial s} - \frac{\partial(s I_s)}{\partial s} - s \frac{\partial I_z}{\partial z} \quad (8)$$

since c_z is independent of z . By expanding all quantities into a complex Fourier series in azimuthal wavenumbers $m > 0$, u_ϕ can easily be recovered using $\partial u_\phi / \partial \phi = im u_\phi$ for each mode.

In both regions I and II, if \mathbf{f} is smooth then so is $I_{s, \phi, z}$. It follows immediately from (3) and (4) that u_s has the same continuity properties as c_s , c_z , and u_z . Furthermore, from (8), continuity of u_ϕ depends on that of u_s and u_z . Thus we may view continuity of all three components of \mathbf{u} (and \mathbf{c}) as depending only on that of u_s . Indeed, (4) and (8), which hold on both sides of \mathcal{C} , show that if u_s has n continuous derivatives (with respect to s) across \mathcal{C} , then u_z has n and u_ϕ has $n - 1$ continuous derivatives across \mathcal{C} . This idea is significantly expanded upon in Sec. III.

It is worth remarking that the above construction of the meridional flow does not depend on axial symmetry. That is, all longitudinal wavenumber components of u_s and u_z follow directly from (3), (6), and (7) and do not depend on (8). The azimuthal component of flow is quite different: using the machinery above, only the non-axisymmetric component of u_ϕ can be found. Indeed, in order to find its axisymmetric component, although (8) provides no information, the contribution from I_ϕ is known and it is only the geostrophic component of flow, $c_\phi(s)$, that remains unspecified. In this case a further solvability condition known as Taylor's constraint²⁴ arises through taking the average of the azimuthal component of (1) over geostrophic cylinders,

$$\int_{C(s)} f_\phi d\phi dz = 0, \quad (9)$$

where $C(s)$ is any geostrophic cylinder. Unless (9) is satisfied no axisymmetric solution exists.

III. A HIERARCHY OF CONSTRAINTS

A. A series representation

In view of the central role played by u_s in the determination of continuity of all three components of \mathbf{u} , we may define the quantity

$$\tilde{Q}_f(\phi) = \lim_{s \rightarrow r_i^+} u_s^I(s, \phi, z) - \lim_{s \rightarrow r_i^-} u_s^{II}(s, \phi, z) = \lim_{s \rightarrow r_i^+} c_s^I(s, \phi) - \lim_{s \rightarrow r_i^-} c_s^{II}(s, \phi) \quad (10)$$

in which the limits approach r_i in s from above and below; this form may be extended in the obvious way to define step changes in derivatives of u_s . The superscripts indicate the region of definition of each u_s ; by continuity of I_s across \mathcal{C} , the right-hand quantity is independent of z . Since \tilde{Q}_f must depend only on \mathbf{f} (the only free parameter in the problem), considerations of continuity of u_s then translate via \tilde{Q}_f into conditions on \mathbf{f} . In fact, our case is somewhat simpler than this difference of two distinct limits. Since u_s^I is independent of r_i (from (7)), it is continuous across \mathcal{C} and we may consider the quantity

$$Q_f(s, \phi) = u_s^I - u_s^{II} \quad (11)$$

within region II, in which the one-sided limit of $s \rightarrow r_i$ from below is of interest; $\tilde{Q}_f(\phi)$ is simply $\lim_{s \rightarrow r_i^-} Q_f(s, \phi)$. Furthermore, any limiting dependence of Q_f close to \mathcal{C} enters only through the variable $\sqrt{r_i^2 - s^2}$, appearing in (6). Exploiting the above two observations permits the expansion

of Q_f in the Taylor series near \mathcal{C}

$$Q_f(s, \phi) = \sum_{n=0}^{\infty} A_n(\phi) (r_i^2 - s^2)^{n/2}.$$

The lowest term in this series is given by $n = 0$ as, inspecting (6) and (7), u_s is finite in both regions I and II (except possibly at $s = 0$); thus $n < 0$ which would render Q_f singular at $s = r_i$ is not permitted. The first two derivatives of Q_f (providing continuity conditions on u_s and u_z) and sQ_f (providing continuity conditions on u_ϕ by (8)) are given below,

$$\frac{\partial Q_f}{\partial s} = \frac{-s A_1}{(r_i^2 - s^2)^{1/2}} - 2s A_2 + O\left(\sqrt{r_i^2 - s^2}\right), \tag{12}$$

$$\frac{\partial^2 Q_f}{\partial s^2} = \frac{-s^2 A_1}{(r_i^2 - s^2)^{3/2}} + \frac{(3s^2 A_3 - A_1)}{(r_i^2 - s^2)^{1/2}} + 2\left((6s^2 - 2r_i^2) A_4 - A_2\right) + O\left(\sqrt{r_i^2 - s^2}\right), \tag{13}$$

$$\frac{\partial(s Q_f)}{\partial s} = \frac{-s^2 A_1}{(r_i^2 - s^2)^{1/2}} + (A_0 - (3s^2 - r_i^2) A_2) + O\left(\sqrt{r_i^2 - s^2}\right), \tag{14}$$

$$\frac{\partial^2(s Q_f)}{\partial s^2} = \frac{-s^3 A_1}{(r_i^2 - s^2)^{3/2}} + \frac{3s(s^2 A_3 - A_1)}{(r_i^2 - s^2)^{1/2}} + 2s\left((10s^2 - 6r_i^2) A_4 - 3A_2\right) + O\left(\sqrt{r_i^2 - s^2}\right). \tag{15}$$

If the structure of \mathbf{f} is such that $Q_f(r_i, \phi) = 0$, occurring if and only if $A_0(\phi) = 0$, both u_s and u_z are continuous. Higher order zeros of Q_f (stemming from a more constrained structure of \mathbf{f}) bestow more continuity on \mathbf{u} . For example, if the further condition $\partial(s Q_f)/\partial s = 0$ is imposed on \mathcal{C} , requiring that $A_1 = 0$ (annulling the singularity in (14)) and $A_0 = 2r_i^2 A_2$, then u_ϕ is additionally continuous. Note that $Q_f = \partial(s Q_f)/\partial s = 0$ also gives $\partial Q_f/\partial s = 0$ which then provides continuity of $\partial u_s/\partial s$ and $\partial u_z/\partial s$. Overall then, continuity of all three components of \mathbf{u} requires $A_0 = A_1 = A_2 = 0$.

We define a hierarchy of conditions that leads to u_s becoming progressively more smooth on \mathcal{C} , to be the ordered list $A_i(\phi) = 0, i = 0, 1, 2, \dots, \infty$; increasing smoothness of u_z and u_ϕ follows immediately as discussed above. The upper section of Table I summarises the continuity of \mathbf{u} on \mathcal{C} with both necessary and sufficient conditions that must be satisfied by the A_n ; in each row, we assume

TABLE I. Hierarchy of continuity conditions satisfied by \mathbf{u} on the tangent cylinder \mathcal{C} with the associated constraints on the expansion coefficients A_n (each being dependent on the forcing \mathbf{f}). Each constraint is only active for one equatorial symmetry of \mathbf{f} (discussed in Secs. III B and III C), as shown in column three. In the upper part of the table, the constraints on the meridional flow u_s and u_z must hold for all wavenumbers $m \geq 0$ individually; those for the azimuthal flow u_ϕ only need hold for the non-axisymmetric components $m > 0$, u_ϕ being undetermined in the axisymmetric case. In the lower part of the table, other continuity conditions are summarised.

Smoothness condition on \mathcal{C}	Constraints	Symmetry
Finiteness of u_s, u_z	Automatically satisfied	
Continuity of u_s, u_z ^a	$A_0 = 0$	E^S
Finiteness of $\frac{\partial u_s}{\partial s}, \frac{\partial u_z}{\partial s}$, and u_ϕ	$A_1 = 0$	E^A
Continuity of $\frac{\partial u_s}{\partial s}, \frac{\partial u_z}{\partial s}$, and u_ϕ	$A_2 = 0$	E^S
Finiteness of $\frac{\partial^2 u_s}{\partial s^2}, \frac{\partial^2 u_z}{\partial s^2}$, and $\frac{\partial u_\phi}{\partial s}$	$A_3 = 0$	E^A
Continuity of $\frac{\partial^2 u_s}{\partial s^2}, \frac{\partial^2 u_z}{\partial s^2}$, and $\frac{\partial u_\phi}{\partial s}$	$A_4 = 0$	E^S
Axisymmetric solution exists	Taylor's constraint	$m = 0, E^S$
Finiteness of \mathbf{u} at $s = 0$	Automatically satisfied	

^aIf $A_1 \neq 0$, then u_ϕ is sufficiently singular on \mathcal{C} to render the kinetic energy of the flow infinite.

that all lower order constraints are satisfied. That is, if $A_n = 0$ then $A_j = 0, j = 0, 1, \dots, n - 1$ are implicitly assumed to hold. This makes intuitive sense: in order to discuss (say) continuity of $\partial u_s / \partial s$, it is reasonable to require that not only is this quantity finite on \mathcal{C} , but that all lower order derivatives, in this case only u_s , are themselves finite and continuous. As will be shown in Subsections III B and III C, each constraint in this hierarchy involves only one “active” equatorial symmetry class, shown in column three of Table I. The lower section of the table provides a statement of finiteness of \mathbf{u} on the axis $s = 0$; this is proved in Sec. III E.

To ensure that all three components of \mathbf{u} are continuous on \mathcal{C} , it is required that $A_0 = A_1 = A_2 = 0$; continuity of $\partial \mathbf{u} / \partial s$ on \mathcal{C} further requires $A_3 = A_4 = 0$. Interestingly, if $A_1 \neq 0$ then the singularity of u_ϕ on \mathcal{C} is sufficiently strong to render the kinetic energy of the flow infinite. This can be easily seen by noting that if $u_s \sim (r_i^2 - s^2)^{1/2}$, then $u_\phi \sim (r_i^2 - s^2)^{-1/2}$, and $|\mathbf{u}|^2 \sim (r_i^2 - s^2)^{-1}$ which has a divergent integral over the spherical shell.

Within our hierarchical structure, we note explicitly that any increment in the level of smoothness imposed on \mathbf{u} introduces only a single further homogeneous constraint $A_n = 0$ (say); this is because the relevant derivative of Q_f involves terms which are homogeneous linear functions of $A_j, j = 0, 1, \dots, n - 1$, and if all lower order constraints are assumed satisfied then A_n must vanish. Further, we remark that as ever higher derivatives of Q_f are constrained to vanish, any given derivative of a component of flow progresses from being singular, to finite but discontinuous, to continuous on \mathcal{C} . Finally, we note that it is possible (although non-intuitive) to construct examples in which this hierarchy is not followed. Consider, for instance, a case where $4r_i^2 A_4 - 3A_2 = 0, A_1 = A_3 = 0$, but $A_4 \neq 0 \neq A_2$. This corresponds to an example in which $\partial u_\phi / \partial s$ is continuous but u_ϕ may be itself discontinuous.

The determination of the coefficients A_n , which depend on which equatorial symmetry is under consideration, is greatly facilitated by computer algebra. To find A_0 , we simply need to evaluate Q_f at $s = r_i$. We find a general A_n by an inductive argument, which is simply the limit of the quotient

$$\frac{Q_f - \sum_{j=0}^{n-1} A_j (r_i^2 - s^2)^{j/2}}{(r_i^2 - s^2)^{n/2}}$$

as $s \rightarrow r_i$ from below, assuming that the $A_j, j < n$, are already known. For $n > 0$ both the numerator and denominator of the above quotient vanish and the limit is undefined, although may be evaluated by using L'Hôpital's rule to evaluate the quotient of the derivatives. However, for $n > 1$, a single application of L'Hôpital's rule is insufficient and the limit remains undefined; empirically we find that the rule must be used n times to find A_n (assisted by re-expressing intermediate expressions in terms of a new numerator and denominator at each stage); see the Appendix for more details.

B. Equatorially symmetric coefficients

In this subsection and in III C we supply the first five terms of the series expansion for Q_f in terms of A_n for each equatorial symmetry class. For typographic purposes, we suppress not only the (s, ϕ, z) dependence of all quantities appearing in the integrands, but also the dependency on ϕ of the boundary terms. For each symmetry class we give the full representation of the series coefficients A_n , not including any simplifications that may arise if all lower order constraints are simultaneously satisfied.

We begin by considering the equatorially symmetric class, this being the symmetry discussed by Hollerbach and Proctor.¹⁰ If \mathbf{f} is E^S , then \mathbf{L} is E^A and \mathbf{u} is E^S . From (6), (7), and (11), the quantity Q_f can be written

$$Q_f = \frac{z_o(z_i + z_o)}{s(r_o^2 - r_i^2)} \left(\int_{z_i}^{z_o} [z_i L_z(s, z) + s L_s(s, z)] dz + (z_o - z_i) \int_0^{z_o} L_z(s, z) dz \right). \quad (16)$$

The first five expansion coefficients are given by

$$\begin{aligned}
 r_i A_0 &= \int_0^\zeta (\zeta L_z + r_i L_s) dz, \\
 \zeta A_1 &= A_0, \\
 2\zeta^2 r_i^3 A_2 &= \int_0^\zeta \left[2r_i^3 L_s + \zeta (3r_i^2 + \zeta^2) L_z - r_i^2 \zeta^2 \frac{\partial L_s}{\partial s} - r_i \zeta^3 \frac{\partial L_z}{\partial s} \right] dz + \\
 &\quad \zeta r_i^2 (r_i L_s(r_i, \zeta) + \zeta L_z(r_i, \zeta)) - r_i^3 \zeta^2 \frac{\partial L_s}{\partial z}(r_i, 0) - 2r_i^2 \zeta^2 L_z(r_i, 0), \\
 2\zeta^3 A_3 &= 2\zeta^2 A_2 - A_0, \\
 24\zeta^3 r_i^5 A_4 &= 3 \int_0^\zeta \left[3r_i^4 L_z - 3\zeta^2 r_i (\zeta^2 + 2r_i^2) \frac{\partial L_z}{\partial s} + r_i^2 \zeta^4 \frac{\partial^2 L_z}{\partial s^2} - \right. \\
 &\quad \left. (4\zeta r_i^4 + \zeta^3 r_i^2) \frac{\partial L_s}{\partial s} + r_i^3 \zeta^3 \frac{\partial^2 L_s}{\partial s^2} \right] dz + \\
 &\quad + 12\zeta^3 r_i^3 \frac{\partial L_z}{\partial s}(r_i, 0) - 12r_i^2 \zeta (2r_i^2 + \zeta^2) L_z(r_i, 0) - 12\zeta r_i^5 \frac{\partial L_s}{\partial z}(r_i, 0) \\
 &\quad + 6\zeta^3 r_i^4 \frac{\partial^2 L_s}{\partial z \partial s}(r_i, 0) - \zeta^3 r_i^5 \frac{\partial^3 L_s}{\partial z^3}(r_i, 0) - 4r_i^4 \zeta^3 \frac{\partial^2 L_z}{\partial z^2}(r_i, 0) \\
 &\quad + 9r_i^5 L_s(r_i, \zeta) - 6\zeta^3 r_i^3 \frac{\partial L_z}{\partial s}(r_i, \zeta) + 3\zeta^2 r_i^4 \frac{\partial L_z}{\partial z}(r_i, \zeta) \\
 &\quad + 3\zeta r_i^5 \frac{\partial L_s}{\partial z}(r_i, \zeta) - 6\zeta^2 r_i^4 \frac{\partial L_s}{\partial s}(r_i, \zeta) + 3r_i^2 \zeta (5r_i^2 + 2\zeta^2) L_z(r_i, \zeta), \quad (17)
 \end{aligned}$$

where $\zeta = \sqrt{r_o^2 - r_i^2}$. In the above, we have used the equatorial symmetry imposing that $L_s(s, \phi, z)$ is an odd function of z and $L_z(s, \phi, z)$ is even to simplify the above expressions. Note that A_3 is a homogeneous function of (A_2, A_0) and A_1 a homogeneous function of A_0 .

In this symmetry, u_s (and therefore) u_z are discontinuous unless the constraint of Hollerbach and Proctor¹⁰ is satisfied:

$$\int_0^\zeta (\zeta L_z + r_i L_s) dz = 0. \quad (18)$$

They conjectured that satisfaction of (18) leads not only to continuity of u_s but removal of any singular behaviour in u_ϕ on \mathcal{C} . Here, we confirm this by noting that since $A_1 = \zeta A_0$, it is clear that if $A_0 = 0$ (giving continuity of u_s) then also $A_1 = 0$ giving finiteness of u_ϕ automatically.

Furthermore, since A_3 depends homogeneously on A_2 and A_0 , it follows that if $A_0 = A_1 = A_2 = 0$ (granting continuity of \mathbf{u}), this automatically renders $A_3 = 0$ and $\partial u_\phi / \partial s$ finite (but not necessarily continuous). We speculate that A_{2n+1} is linearly and homogeneously dependent on A_{2k} , $k < n$, so that $A_{2n+1} = 0$ automatically if all lower order constraints are satisfied; that is, within this symmetry class, only $A_{2n} = 0$ are active constraints.

C. Equatorially antisymmetric coefficients

If \mathbf{f} is E^A , then \mathbf{L} is E^S and \mathbf{u} is E^A ; the quantity Q_f can then be written

$$Q_f = \frac{z_i + z_o}{s(r_o^2 - r_i^2)} \left(z_o \int_{z_i}^{z_o} [z_i L_z(s, z) + s L_s(s, z)] dz + s (z_i - z_o) \int_0^{z_o} L_s(s, z) dz \right). \quad (19)$$

The first five series coefficients A_n are then given by

$$\begin{aligned}
 A_0 &= 0, \\
 r_i \zeta A_1 &= \int_0^\zeta (\zeta L_z + r_i L_s) dz - r_i \zeta L_s(r_i, 0), \\
 \zeta A_2 &= A_1, \\
 6 \zeta^3 r_i^3 A_3 &= 3 \int_0^\zeta \left[r_i^3 L_s + \zeta (2r_i^2 + \zeta^2) L_z - \zeta^2 r_i^2 \frac{\partial L_s}{\partial s} - r_i \zeta^3 \frac{\partial L_z}{\partial s} \right] dz + \\
 &\quad 3 \zeta r_i^2 (r_i L_s(r_i, \zeta) + \zeta L_z(r_i, \zeta)) - \\
 &\quad 6 \zeta r_i^3 L_s(r_i, 0) + 3 \zeta^3 r_i^2 \frac{\partial L_s}{\partial s}(r_i, 0) - 3 \zeta^3 r_i^2 \frac{\partial L_z}{\partial z}(r_i, 0) - \zeta^3 r_i^3 \frac{\partial^2 L_s}{\partial z^2}(r_i, 0), \\
 2 \zeta^3 A_4 &= 2 \zeta^2 A_3 - A_1. \tag{20}
 \end{aligned}$$

As before, we have used the equatorial symmetry of \mathbf{L} to simplify the expressions, exploiting the fact that $L_s(s, \phi, z)$ is an even function of z and $L_z(s, \phi, z)$ is odd. Note that A_4 is a homogeneous function of (A_3, A_1) and A_2 a homogeneous function of A_1 . Thus it would appear that the conditions A_{2n} are automatically satisfied (assuming that all lower order constraints are satisfied) and so only the constraints $A_{2n+1} = 0$ are active within this symmetry class.

In this symmetry, $A_0 \equiv 0$ and so both u_s and u_z are automatically continuous on \mathcal{C} . This occurs because $u_s = 0$ at $z = 0$ on either side of \mathcal{C} : in region II, stemming from the non-penetration condition there, and in region I from the symmetry imposed. The behaviour of u_ϕ is tied to $\partial(s Q_t)/\partial s$ and requires $A_1 = 0$ to avoid singular behaviour. In fact, since $A_1 = \zeta A_2$, this condition is also sufficient to ensure that $A_2 = 0$ and so renders u_ϕ continuous. Thus, in this symmetry class, finiteness of both u_ϕ and $\partial u_s/\partial s$ implies also continuity of these quantities.

D. Comparison of the symmetry classes

Having derived the first few of the hierarchy of constraints for each equatorial symmetry class individually, we briefly remark on some general characteristics. First, although we only listed the coefficients A_n for $n \leq 4$, it is striking that if \mathbf{u} is E^S (E^A) and n is an odd (even) integer, then A_n is linearly and homogeneously related to the A_j for $j < n$ and j is even (odd). In this sense, the hierarchy of constraints $\{A_n = 0\}$ exactly partitions between the two symmetry classes: the E^S symmetry only requiring consideration of A_{2n} , and the E^A symmetry consideration only of A_{2n+1} (see column three of Table I). Additionally, it cannot be the case that a threshold K is reached such that A_k is homogeneously dependent on A_j for any $k > K, j \leq K$ (that is, progressing further down the series of A_j fails to produce any more constraints), since as n is increased ever higher derivatives are introduced which cannot be expressed in terms of those of lower degrees (as can be seen, for example, in (17)).

Second, there appear to be strong links between the coefficients A_n from different symmetry classes. Perhaps most apparent is the homogeneous relations satisfied between coefficients being almost independent of symmetry class (but offset by one in the index n). For instance, it is striking to compare the relation for A_1 and A_3 in the E^S class with those for A_2 and A_4 in the E^A class. Further, it is interesting to compare the expressions for coefficients associated with the active constraints, for example, A_2 in the E^S class and A_3 in E^A . Aside from the boundary terms evaluated on the equator (whose form is different, owing to the different behaviour that the two symmetry classes impart), all remaining terms are analytically identical *if* the preceding constraints are satisfied. For example, in the E^S symmetry class, it is easy to show that if $A_0 = 0$ then the integral terms in A_2 coincide (within a constant factor) with those with A_3 from the E^A class, as do the outer-sphere boundary terms. We speculate that the relations described above, motivated by the very restricted set of coefficients A_n presented, continue to hold for any integer n .

E. Finiteness on the rotation axis

The rotation axis is a singular location in cylindrical coordinates and it is of interest to clarify whether or not \mathbf{u} is guaranteed to be finite on the axis if \mathbf{f} is everywhere smooth. Inspecting (1), it would seem likely that a singularity of \mathbf{u} is inconsistent with the other (non singular terms) of the equation; here, we briefly prove that this is indeed the case.

We will assume that \mathbf{f} is smooth everywhere, which means that $I_{s, \phi, z}$ is also smooth and so the behaviour of \mathbf{u} yet again hinges on that of \mathbf{c} .

From (6), c_z is continuous as $s \rightarrow 0$ and attains the finite value

$$\frac{r_i}{r_o - r_i} \int_{r_i}^{r_o} L_z(0, z) dz$$

at $s = 0$. Furthermore, as shown by (8), finiteness of u_ϕ as $s \rightarrow 0$ depends only on the behaviour of $\partial(s c_s)/\partial s$ and from (6) attains the finite value

$$\frac{r_o}{r_i - r_o} \int_{r_i}^{r_o} \left[r_i \frac{\partial L_z}{\partial s}(0, z) + L_s(0, z) \right] dz$$

at $s = 0$. It remains to show that c_s is finite on the axis.

Finiteness of c_s is not immediately assured as, from (6), as $s \rightarrow 0$:

$$c_s(s, \phi) = \frac{r_o r_i}{(r_i - r_o)} \int_{r_i}^{r_o} \frac{L_z(s, z)}{s} dz + O(1) \tag{21}$$

and we require that the integral above remains finite.

However, \mathbf{L} is a smooth vector field and therefore L_z is a smooth scalar. Standard regularity conditions¹ then permit the expansion

$$L_z = \sum_{m=0}^{\infty} \sum_{n=0}^{\infty} A_{m,n}(z) s^{m+2n} e^{i m \phi} \tag{22}$$

and therefore (21) is guaranteed to be finite when $m > 0$. In the axisymmetric case, we may write $2 L_z = (\nabla \times \mathbf{f})_z = \frac{1}{s} \frac{\partial}{\partial s}(s f_\phi)$ and thus need to show that

$$\int_{z_i}^{z_o} \frac{1}{s^2} \frac{\partial}{\partial s}(s f_\phi) dz = \frac{1}{s^2} \int_{z_i}^{z_o} f_\phi dz + \frac{1}{s} \int_{z_i}^{z_o} \frac{\partial f_\phi}{\partial s} dz \tag{23}$$

has a finite limit as $s \rightarrow 0$. By (9), the first integral on the right hand side is zero for all s and thus the first term on the right is identically zero. Since (9) is valid for all s , we may differentiate it to show that

$$0 = \frac{d}{ds} \int_{z_i}^{z_o} f_\phi dz = \int_{r_i}^{r_o} \frac{\partial f_\phi}{\partial s}(0, z) d\phi dz + O(s) \tag{24}$$

as $s \rightarrow 0$ where the derivative of the end points contribute the $O(s)$ term. It then follows that the second term on the right hand side of (23) is $O(1)$ and therefore finite as $s \rightarrow 0$.

IV. EXAMPLES

In this section we present some simple examples of forcings that satisfy a small number of the derived constraints, illustrating the different levels of continuity bestowed on the flow. We fix the inner and outer radii to be 1/2 and 3/2, respectively. We first remark that, in addition to the equatorial symmetry already discussed, any vector of azimuthal wavenumber $m > 0$ that possesses cylindrical components behaving as

$$[s^{m+1} f(s^2, z), s^{m+1} g(s^2, z), s^m h(s^2, z)],$$

where f, g , and h are arbitrary smooth functions, is guaranteed to be everywhere smooth, i.e., infinitely differentiable (including on the z axis).¹⁴ This will constrain our forcings \mathbf{f} when choosing examples.

TABLE II. For the example in the E^S symmetry class, the addition of free parameters into the forcing allows an increasing number of constraints to be satisfied.

a_0	a_1	a_2	Constraints satisfied
0	0	0	None
-7	0	0	$A_0 = A_1 = 0$
-53/4	25	0	$A_0 = A_1 = A_2 = A_3 = 0$
-315/16	153/2	-103	$A_0 = A_1 = A_2 = A_3 = A_4 (=A_5) = 0$

Before embarking on the more general case, it is worth remarking that if \mathbf{f} is both E^A and independent of z , then $L_z = 0$ since it is simultaneously both odd in z and independent of z . It follows immediately from (19) that $Q_f \equiv 0$ and *all* derivatives of \mathbf{u} are automatically continuous across \mathcal{C} . We have not identified any such simple form of \mathbf{f} that produces smooth flows in the E^S symmetry.

We now present a family of non-trivial low-degree examples in each equatorial symmetry class. Consider the forcing

$$\mathbf{f} = \left[s^2(1+z^2) + s^4 z^2 \sum_{k=0}^K a_k s^{2k} \right] \cos \phi \hat{\mathbf{s}} + s z \cos \phi \hat{\mathbf{z}} \quad (25)$$

which drives an E^S flow of the form

$$(u_s, u_\phi, u_z) = (\tilde{u}_s(s, z) \sin \phi, \tilde{u}_\phi(s, z) \cos \phi, \tilde{u}_z(s, z) \sin \phi). \quad (26)$$

Note the azimuthal phase shift between \mathbf{f} and \mathbf{u} . We may choose the coefficients a_k to satisfy the constraints A_n . Table II shows how by adding in extra degrees of freedom, more constraints can be satisfied. For instance, choosing $K = -1$ (so that there are no degrees of freedom in \mathbf{f}) violates all constraints A_n and thus u_s, u_z are discontinuous, and u_ϕ singular on \mathcal{C} . If $K = 0$, then if $a_0 = -7$, $A_0 = A_1 = 0$ and so u_s, u_z become continuous and u_ϕ finite (but discontinuous) on \mathcal{C} . Contour plots of $\tilde{u}_s, \tilde{u}_\phi$, and \tilde{u}_z for these two cases (rows one and two of Table II) are shown in the first two rows of Figure 2. Note that, following the observations in Sec. III D, each additional free parameter allows two more constraints to be satisfied as only half the constraints are active for any equatorial symmetry; we therefore anticipate that A_5 is also rendered zero in the last row.

As a second example, consider the forcing

$$\mathbf{f} = s^2 z \cos \phi \hat{\mathbf{s}} + \left[s(1+z^2) + s^3 z^2 \sum_{k=0}^K a_k s^{2k} \right] \cos \phi \hat{\mathbf{z}}$$

which drives an E^A flow of the form (26) and is, within some factors of s , the E^S forcing with the s and z components interchanged. This time, $A_0 = 0$ irrespective of \mathbf{f} so that the first constraint is satisfied with no degrees of freedom. When $K = 0$ we may satisfy not only $A_1 = 0$ but also $A_2 = 0$ (since A_2 is proportional to A_1). Table III summarises how an increasing number of constraints may become satisfied when admitting more degrees of freedom. Contour plots corresponding to the first two rows of this table are shown as rows three and four of Figure 2.

TABLE III. Similar to Table II caption, but for the E^A symmetry example.

a_0	a_1	Constraints satisfied
0	0	$A_0 = 0$
2	0	$A_0 = A_1 = A_2 = 0$
4	-8	$A_0 = A_1 = A_2 = A_3 = A_4 = 0$

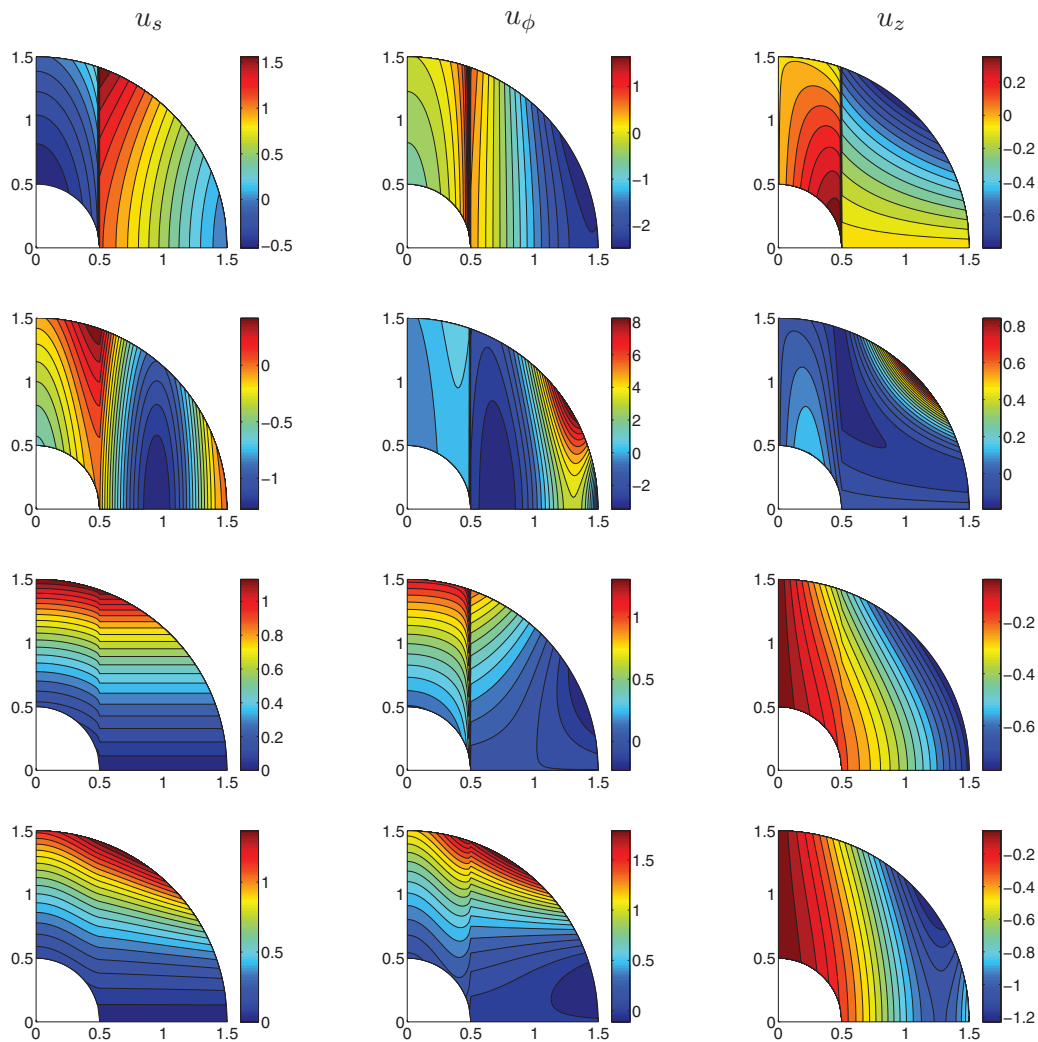


FIG. 2. Contour plots in (s, z) of $(\tilde{u}_s, \tilde{u}_\phi, \tilde{u}_z)$, the meridional profile of the components of \mathbf{u} , which are E^S (rows 1 and 2) and E^A (rows 3 and 4), corresponding to the examples in the text. In row 1, the forcing has no free parameters and violates all constraints on \mathcal{C} ; thus u_s and u_z are discontinuous (but finite) and u_ϕ is singular. In row 2, admitting a single degree of freedom allows $A_0 = A_1 = 0$ rendering u_s and u_z continuous and u_ϕ discontinuous (but finite) on \mathcal{C} . In row 3, the forcing has no degrees of freedom but automatically satisfies $A_0 = 0$ rendering u_s and u_z continuous but u_ϕ singular on \mathcal{C} . In row 4, a single degree of freedom allows $A_0 = A_1 = A_2 = 0$ which renders u_s and u_z differentiable and u_ϕ continuous.

V. THE EFFECT OF VISCOSITY

In this section we consider in what manner viscosity smoothes out any singularity or discontinuity in the flow into shear layers of finite thickness. We solve

$$2\mathbf{k} \times \mathbf{u} - E\nabla^2 \mathbf{u} = -\nabla p + \mathbf{f} \quad (27)$$

numerically in the spherical-shell subject to nonslip boundary conditions, using a fully spectral method based on spherical harmonics and Chebyshev polynomials. Although spectral methods are not in general the method of choice for representing functions which are not smooth, the results will show that the viscous calculations converge to the inviscid case provided they are adequately

resolved. We write

$$\mathbf{u} = \nabla \times \left[t(r, \theta) e^{i\phi} \hat{\mathbf{r}} \right] + \nabla \times \nabla \times \left[s(r, \theta) e^{i\phi} \hat{\mathbf{r}} \right],$$

where each of the toroidal and poloidal scalar functions are further decomposed as, for instance,

$$t(r, \theta) = \sum_{k=1}^{K_{max}} \sum_{n=0}^{N_{max}} t_{k,n} P_{2k-1}^1(\cos \theta) T_n(x), \quad s(r, \theta) = \sum_{k=1}^{K_{max}} \sum_{n=0}^{N_{max}} s_{k,n} P_{2k}^1(\cos \theta) T_n(x),$$

where P_n^m is an associated Legendre function and $T_n(x)$ is a Chebyshev polynomial. The radial coordinate is stretched so that $x = 2r - 2$ satisfies $-1 \leq x \leq 1$ over the spherical-shell domain $1/2 \leq r \leq 3/2$. The representation above exploits the fact that (27) separates both in azimuthal mode and equatorial symmetry. The expression written above, involving P_n^m with $n - m$ even for the toroidal scalar and $n - m$ odd for the poloidal scalar is equatorially antisymmetric. Similar representations exist for the equatorially symmetric solutions. After projecting each term of the (linear) Eq. (27) back onto the spectral basis,⁹ the matrix-vector system, for the coefficients $(t_{k,n}; s_{k,n})$, may be found using standard Numerical Algorithms Group library routines on a shared-memory machine. Note that the solution is found directly, rather than as a perturbation to a given (e.g., the inviscid) background state. We found that for values of Ekman number $E = 10^{-7}$, $E = 10^{-8}$, and $E = 10^{-9}$, sufficient resolutions were given by $K_{max} = N_{max}$ of 400, 600, and 800, respectively, for converged solutions. By equatorial symmetry, the largest spherical harmonic degree used is $L_{max} = 2K_{max}$, taking a maximum value of 1600. Although the matrix required to be inverted is of banded structure, at this highest truncation the inversion routines took 19 hours to run and required in total around 92 Gb of memory (including all overhead), close to the upper limit of our available computational resources. We therefore did not attempt to find solutions at higher truncations than this.

It is worth remarking that although the operator $\nabla^2 \mathbf{u}$ leaves invariant not only the azimuthal wavenumber but the azimuthal phase of \mathbf{u} , the viscous solutions do not remain of the simple form (26). This is because (27) combines the Coriolis operator $\hat{\mathbf{k}} \times$ that swaps the azimuthal phase (compare (26) to (25)) and ∇^2 which does not, so the solution must be a mixture of phases. As $E \rightarrow 0$ however, any components of \mathbf{u} out of phase with solutions of the form (26) will reduce to zero.

Figure 3 compares cross sections of the flow components $(\tilde{u}_s, \tilde{u}_\phi, \tilde{u}_z)$, derived using low-viscosity, and the formally inviscid solution. We show only the component of the viscous solutions of the form (26). The systems are driven by the equatorially symmetric body force of Sec. IV that satisfies no constraints. As viscosity is decreased from $E = 10^{-7}$ (top row), $E = 10^{-8}$ (middle row) to $E = 10^{-9}$ (bottom row), all three components of flow converge to the formally inviscid solution shown in the top row of Figure 2. This plot also confirms that the boundary layers on either spherical boundary (owing to the nonslip conditions imposed) have no influence on the free-stream solution.

A more detailed view of the shear layers is afforded by cut-through sections at $z = 1$, midway between r_i and r_o . Figure 4 examines \tilde{u}_ϕ (leftmost plots) for our most singular examples (i.e., driven by forces that satisfy no constraints) for both the equatorially symmetric (top row) and antisymmetric (bottom row) symmetries. It is apparent that, as E decreases, the viscous solutions (colour) converge to the formally inviscid solution (black) which is singular at $s = r_i = 1/2$. Interestingly, viscosity smoothes the singularity in u_ϕ into a boundary layer centred on the tangent cylinder in which the peak shear is located either outside (inside) the tangent cylinder in the equatorially symmetric (antisymmetric) symmetry class.

Motivated by some of the known asymptotic scalings in both the boundary-driven²² and force-driven²¹ problems, we plot suitably rescaled solutions in the panels on the right. In both rows, the coincidence of the horizontal location of features a' to f' , rescaled from features a to f , supplies strong numerical evidence of inner and outer boundary layers of respective thickness $E^{2/7}$ and $E^{1/4}$. For the E^S symmetry, u_ϕ apparently scales as $E^{-1/3}$ within both boundary layers (as indicated by the z -coordinate of features a' to c'). In the E^A symmetry, the leftmost plot shows that the solution in the outer boundary-layer scales independently of E (feature f). The scaling in the z -direction suggests

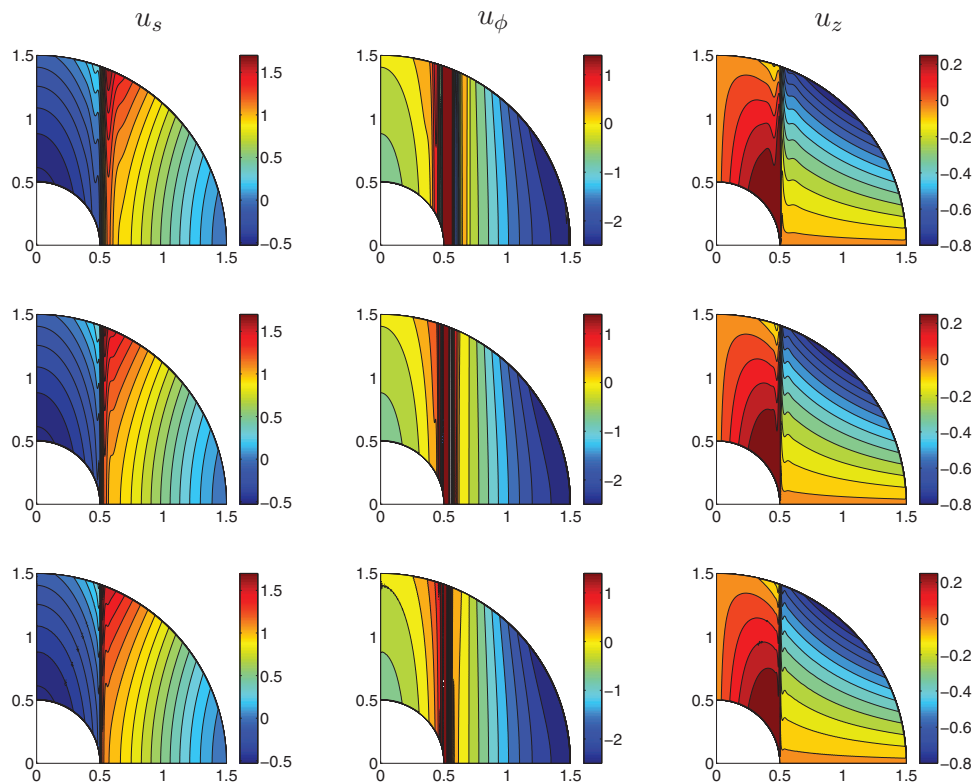


FIG. 3. Contour plots in (s, z) of $(\tilde{u}_s, \tilde{u}_\phi, \tilde{u}_z)$, the meridional profile of the components of \mathbf{u} of the form (26), at $E = 10^{-7}$ (top), $E = 10^{-8}$ (middle), and $E = 10^{-9}$ (bottom) for the E^S example which satisfies no constraints. As viscosity is decreased, the development of the shear layer in u_ϕ outside \mathcal{C} becomes apparent. The inviscid solution to which these converge is shown in the top row of Figure 2.

that the inner solution scales as $O(E^{1/20})$ (feature d'), although the peak values e' do not then coincide. The inset shows a z -scaling of $E^{1/10}$ in which feature e'' appears to become independent of E . This more complex profile suggests a nested structure of boundary layers, in which the solution takes magnitudes $E^{-1/20}$, $E^{-1/10}$, and $O(1)$ as s increases across \mathcal{C} . Lastly, we remark that within boundary-layer theory as a whole, the scalings of $E^{-1/20}$ and $E^{-1/10}$ are not particularly commonplace and, in view of their empirical determination, the reader may wonder about the accuracy of the exponents we provide. Although they are the best fit to our data within our range $E \geq 10^{-9}$, any scalings of the form $E^{-1/k}$, $16 \leq k \leq 24$ or $E^{-1/k}$, $9 \leq k \leq 12$, respectively, are (broadly speaking) not inconsistent with the numerical calculations. It is likely that an accurate determination of the scalings will only emerge through a rigorous boundary-layer analysis.

VI. DISCUSSION

In this paper, we have described the analytic solution to a steady fluid driven by a body force \mathbf{f} in a rotating spherical shell, in the absence of viscosity and inertia. Essentially, in what may be viewed as a generalisation of the Taylor-Proudman theorem, the impenetrable boundary conditions on the inner sphere are communicated only in the direction parallel to the rotation axis and this leads to singularities or discontinuities in all components of the driven flow on the tangent cylinder, \mathcal{C} . We have set out a hierarchy of conditions, imposed on the body force \mathbf{f} , that progressively smoothes the driven flow on \mathcal{C} . The first condition, $A_0 = 0$, ensures that u_s is continuous, the second, $A_1 = 0$, removes the singularity in u_ϕ and if $A_0 = A_1 = A_2 = 0$ then all three components of the flow are continuous. This hierarchy of conditions on \mathbf{f} is analogous to the nested sequence of boundary layers found in similar problems that retain a small viscosity,^{12,22} each additional layer removing a higher

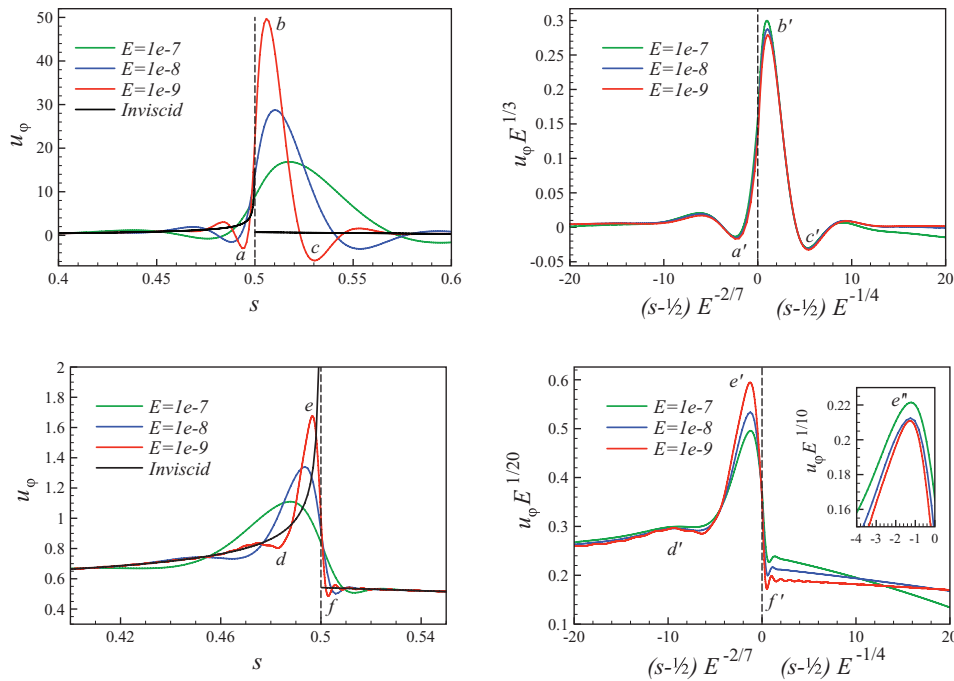


FIG. 4. Cut through at $z = 1$ of \tilde{u}_ϕ , the meridional profile of u_ϕ of the form (26), of the E^S (top row) and E^A (bottom row) example cases produced by \mathbf{f} that satisfies no constraints on \mathcal{C} , showing how the singularities are smoothed by viscosity into shear layers of finite thickness. The leftmost plots show the raw numerical solution for three different Ekman numbers (colour) and the analytic inviscid solution in black; the rightmost plots show rescaled solutions as indicated by the axes. In both symmetries, the viscous boundary layers appear to have lateral extent $E^{2/7}$ and $E^{1/4}$, respectively, inside and outside the tangent cylinder, as suggested by the independence in E of the horizontal position of the features d' to f' , rescaled from a to f . For the E^S symmetry, the magnitude of u_ϕ appears to scale as $E^{-1/3}$ everywhere close to \mathcal{C} and takes its peak value in the shear layer outside \mathcal{C} . In the E^A symmetry, u_ϕ attains its maximum value inside \mathcal{C} and appears to scale as $O(1)$ in the outermost layer (feature f), $O(E^{-1/20})$ in the innermost (feature d'), and $O(E^{-1/10})$ in a mid-layer (feature e'' as shown in the inset).

order discontinuity from the flow. In the inviscid case considered, a smooth flow (i.e., infinitely differentiable) on \mathcal{C} must be driven by a force satisfying infinitely many constraints. Analogously, in the viscously adjusted problem, a smooth flow would require an infinite sequence of boundary layers, each ensuring the continuity of ever higher derivatives.

In this paper we have taken \mathbf{f} to be prescribed; but in general, it will be time-dependent, comprising buoyancy and the magnetic Lorentz force. It is this latter ingredient that, through the resistance to shearing motion by the magnetic field lines, we anticipate will adjust \mathbf{f} to satisfy as many constraints as is dynamically demanded. In the equatorially symmetric case, Hollerbach⁷ has already shown that indeed \mathbf{f} is perturbed to ensure that $A_0 = A_1 = 0$, providing continuity of u_s and removing the discontinuity in u_ϕ . How many more smoothness constraints are implicitly satisfied by the action of the magnetic field remains an open question although this is currently being investigated.

The influence of magnetic fields and their smoothing effect on shear layers may have significant consequences for the dynamics of the Earth's core. So-called torsional waves, motions of axially symmetric cylinders of fluid connected by magnetic field lines, have been predicted both theoretically^{2,24} and are supported by mounting observational evidence.^{6,11} One interesting aspect of the latter study, corroborated by recent low-viscosity geodynamo simulations²⁵ is that these waves appear to emanate from the tangent cylinder and propagate both radially inwards and outwards. To explain this, we consider a background state of the core in which the body force satisfies enough of the constraints to ensure that the flow is (sufficiently) smooth on the tangent cylinder. Fluctuations in this state will cause violations of the constraints; hydrodynamically the system would respond by forming shear layers, but we speculate that the resisting influence of the magnetic field will cause (MHD) waves to propagate away from the tangent cylinder, carrying with them the

problematic disturbance. Within our (principally non-axisymmetric) framework, we must then appeal to nonlinear interactions to produce (axisymmetric) torsional waves. Interestingly, there is evidence that persistent localised shear layers could spawn other observed instabilities such as geomagnetic jerks.¹⁷

Even without the influence of a magnetic field, by reinstating linearised inertia, $R_o \partial \mathbf{u} / \partial t$, it is likely still possible to obtain hydrodynamic waves propagating from the tangent cylinder. Consider the time-dependent problem in which the initial flow is quiescent (in the rotating frame) and is at all times driven by a steady body force \mathbf{f} that satisfies no constraints. Assuming that the set of inertial modes (solutions of the homogeneous equation given by $\mathbf{f} = \mathbf{0}$) are complete, then the full-solution is simply the discontinuous/singular flow along with an infinite linear sum of inertial modes required to match the initial condition. The shortest length-scale modes required on the tangent cylinder, to remove any initial discontinuity or singularity, are associated with the fastest timescales and may effect a wavelike divergence from the tangent cylinder.

It is of interest to compare the constraints that we have derived to that of Taylor,²⁴ particularly in terms of the number of conditions to which each constraint translates within a discretised system. Taylor's constraint states that the azimuthal component of the body force (which reduces to the Lorentz force assuming that buoyancy is purely radial), must vanish when averaged on each geostrophic cylinder. Within a model discretised by spherical harmonics (of maximum degree and order L_{max}) in solid angle and a certain set of polynomials in radius of size L_{max} , the number of conditions enumerates to $O(5L_{max})$.^{15,16} In this study, our constraints involve certain averages of the body force which, although only applying on the tangent cylinder, apply separately to each azimuthal wavenumber $1 \leq m \leq 2L_{max}$ (since \mathbf{f} depends quadratically on the magnetic field). Accounting for both real and imaginary components of each complex exponential mode, these enumerate to a total of $O(4L_{max})$ conditions. Although a very crude comparison, the number of discretised conditions corresponding to both types of constraint scales similarly within such a discretised scheme.

We finish by describing the outstanding issues that remain unresolved. First is the puzzle of why the equatorial symmetry classes are staggered between the constraints, each symmetry class being "active" only in every other constraint in our hierarchy. This mathematical property may well be tied to the remarkable similarity between the algebraic forms of the constraints between the two symmetry classes, whose origin might be revealed by addressing the problem in a different manner.

Second is an understanding of precisely how viscosity smoothes out discontinuities or singularities into a shear layer and its scaling with the Ekman number, E . In our study, we investigated numerically the most singular examples of flows, of both equatorial symmetries, driven by a body force satisfying no constraints. In both cases, the azimuthal component of flow has the same (inviscid) structure $u_\phi \sim (r_i^2 - s^2)^{-1/2}$, although, under equatorial symmetry, the singularity is arguably more severe than in the equatorially antisymmetric case, since u_s and u_z are also discontinuous on \mathcal{C} . Viscosity smoothes this singularity into a shear layer comprising an inner and outer layer on either side of the tangent cylinder. For both symmetries, these inner and outer layers have a thickness that appears to scale as $O(E^{2/7})$ and $O(E^{1/4})$, respectively, scalings identical to the boundary-forced case²² and with numerical studies of inertial waves with weak viscosity.¹⁹ Interestingly, the layer in which the shear takes its peak value depends on the symmetry class: the E^S (E^A) example taking its peak value in the outer (inner) boundary layer. Further, the magnitude of the shear appears to scale differently between the symmetry classes, being of $O(E^{-1/3})$ for E^S and of multiple scalings $O(E^{-1/20})$, $O(E^{-1/10})$ [or thereabouts, see the comments at the end of Sec. V] and $O(1)$ for E^A depending on the position in the boundary-layer system. We have no explanation for this strong dependence on structure with equatorial symmetry, although it is likely to be revealed by a formal asymptotic treatment of the problem. It would further be of interest to investigate the scaling of the boundary layers in which derivatives of the flow change rapidly, when the system is driven by a body force satisfying some non-zero number of constraints.

Lastly, our results have focussed primarily on the non-axisymmetric constraints as a complete discussion of the axisymmetric flow is much more difficult. This is because the geostrophic flow of the form $c_\phi(s)\hat{\phi}$ is formally undetermined by the governing reduced Navier-Stokes equation (1), essentially because $\mathbf{k} \times c_\phi(s)\hat{\phi} = -c_\phi(s)\hat{s}$ which can be absorbed into the pressure gradient. However, by considering the inviscid magnetohydrodynamical system, it is possible to show that

$c_\phi(s)$, both inside and outside the tangent cylinder, must be the solution of certain ordinary differential equations.²⁴ It is not immediately clear what conditions of continuity must be required to match the two solutions on \mathcal{C} , although a resolution of this may lead to a similar hierarchy of constraints for the axisymmetric flow.

ACKNOWLEDGMENTS

P.W.L. would like to acknowledge useful conversations with Glenn Ierley, Andy Jackson, Mike Proctor, Andrew Soward, and Keke Zhang. This work was supported by NERC (Natural Environment Research Council) Grant No. NE/G0140431 and ERC (European Research Council) Grant No. 247303 (“MFECE”). The numerical studies were performed on the supercomputer Brutus at ETH.

APPENDIX: EVALUATION OF EXPANSION COEFFICIENTS

We briefly outline the procedure for calculating the expansion coefficients, A_n , $n \geq 0$, for the E^S symmetry class; the E^A coefficients are derived in an identical fashion. The first term in the expansion, A_0 , is simply Q_f evaluated at $s = r_i$, which gives

$$A_0 = \frac{1}{r_i} \int_0^\zeta (\zeta L_z + r_i L_s) dz.$$

The next coefficient is given by

$$A_1 = \lim_{s \rightarrow r_i} \frac{Q_f - A_0}{(r_i^2 - s^2)^{1/2}}.$$

Since both numerator and denominator are zero in the required limit, we use L’Hôpital’s rule,

$$A_1 = \lim_{s \rightarrow r_i} \frac{d(Q_f - A_0)/ds}{(-s)(r_i^2 - s^2)^{-1/2}} = \frac{A_0}{\zeta} - L_s(r_i, 0),$$

reducing to $\zeta A_1 = A_0$ since, owing to symmetry, L_s is zero at $z = 0$. Hidden in the above equation is some elementary but tedious differentiation, taking account of the fact that not only the integrands but the limits of the integrals appearing in Q_f depend on s ; finding the derivative required above is a task greatly facilitated by computer algebra. A similar procedure is followed to find A_2 ,

$$A_2 = \lim_{s \rightarrow r_i} \frac{Q_f - A_0 - (r_i^2 - s^2)^{1/2} A_1}{(r_i^2 - s^2)}.$$

Since both numerator and denominator are again zero, L’Hôpital’s rule gives

$$A_2 = \lim_{s \rightarrow r_i} \frac{d(Q_f - A_0 - (r_i^2 - s^2)^{1/2} A_1)/ds}{(-2s)}.$$

However, this limit is also undefined and in order to make progress the above quantity can be re-expressed as a new fraction in which both numerator and denominator are zero at $s = r_i$,

$$\frac{H}{2 r_i \zeta s^3 z_i z_0 (z_0 - z_i)},$$

where H is a somewhat lengthy expression involving integrals and boundary terms. Using L’Hôpital’s rule again turns out to give a finite limit at $s = r_i$; the intermediate quantities in the calculation are again lengthy. The coefficient A_3 follows similarly, although we find that we need to apply L’Hôpital’s rule three times, re-expressing the intermediate terms twice. Further coefficients in the expansion follow similarly, and are found by applying L’Hôpital’s rule n -times and re-expressing the intermediate terms $n - 1$ times.

¹J. P. Boyd, *Chebyshev and Fourier Spectral Methods* (Dover, 2001).

²S. I. Braginsky, “Torsional magnetohydrodynamic vibrations in the earth’s core and variations in the length of day,” *Geomagn. Aeron. (Engl. Trans.)* **10**, 1–10 (1970).

- ³U. Christensen and J. Wicht, "Numerical Dynamo Simulations," in *Treatise on Geophysics*, edited by P. Olson (Elsevier, 2007), Vol. 8, pp. 245–279.
- ⁴E. Dormy, P. Cardin, and D. Jault, "MHD flow in a slightly differentially rotating spherical shell, with conducting inner core, in a dipolar magnetic field," *Earth Planet. Sci. Lett.* **160**, 15–30 (1998).
- ⁵D. R. Fearn, "Hydromagnetic flow in planetary cores," *Rep. Prog. Phys.* **61**, 175–235 (1998).
- ⁶N. Gillet, D. Jault, E. Canet, and A. Fournier, "Fast torsional waves and strong magnetic field within the Earth's core," *Nature (London)* **465**(74), 74–77 (2010).
- ⁷R. Hollerbach, "Imposing a magnetic field across a nonaxisymmetric shear layer in a rotating spherical shell," *Phys. Fluids* **6**(7), 2540–2544 (1994).
- ⁸R. Hollerbach, "Magnetohydrodynamic Ekman and Stewartson Layers in a Rotating Spherical Shell," *Proc. R. Soc. London, Ser. A* **444**(1921), 333–346 (1994).
- ⁹R. Hollerbach, "A spectral solution of the magneto-convection equations in spherical geometry," *Int. J. Numer. Methods Fluids* **32**, 773–797 (2000).
- ¹⁰R. Hollerbach and M. R. E. Proctor, "Non-axisymmetric shear layers in a rotating spherical shell," in *Solar and Planetary Dynamos*, edited by Proctor *et al.* (Cambridge University Press, 1993), pp. 145–152.
- ¹¹D. Jault, C. Gire, and J. L. Le Mouél, "Westward drift, core motions and exchanges of angular momentum between core and mantle," *Nature (London)* **333**(26), 353–356 (1988).
- ¹²N. Kleeeorin, I. Rogachevskii, A. Ruzmaikin, A. M. Soward, and S. Starchenko, "Axisymmetric flow between differentially rotating spheres in a dipole magnetic field," *J. Fluid Mech.* **344**, 213–244 (1997).
- ¹³M. Kono and P. H. Roberts, "Recent geodynamo simulations and observations of the geomagnetic field," *Rev. Geophys.* **40**(4), 1013, doi:10.1029/2000RG00102 (2002).
- ¹⁴H. R. Lewis and P. M. Bellan, "Physical constraints on the coefficients of Fourier expansions in cylindrical coordinates," *J. Math. Phys.* **31**(11), 2592–2596 (1990).
- ¹⁵P. Livermore, G. Ierley, and A. Jackson, "The structure of Taylor's constraint in three dimensions," *Proc. R. Soc. London, Ser. A* **464**, 3149–3174 (2008).
- ¹⁶P. Livermore, G. Ierley, and A. Jackson, "The construction of exact Taylor states II: The influence of an inner core," *Phys. Earth Planet. Inter.* **178**, 16–26 (2010).
- ¹⁷L. Petitdemange, E. Dormy, and S. A. Balbus, "Magnetostrophic MRI in the Earth's outer core," *Geophys. Res. Lett.* **35**(L15305), 1–6, doi:10.1029/2008GL034395 (2008).
- ¹⁸I. Proudman, "The almost-rigid rotation of viscous fluid between concentric spheres," *J. Fluid Mech.* **1**(5), 505–516 (1956).
- ¹⁹M. Rieutord and L. Valdettaro, "Inertial waves in a rotating spherical shell," *J. Fluid Mech.* **341**, 77–99 (1997).
- ²⁰X. D. Song and P. G. Richards, "Seismological evidence for differential rotation of the Earth's inner core," *Nature (London)* **382**(6588), 221–224 (1996).
- ²¹A. M. Soward and R. Hollerbach, "Non-axisymmetric magnetohydrodynamic shear layers in a rotating spherical shell," *J. Fluid Mech.* **408**, 239–274 (2000).
- ²²K. Stewartson, "On almost rigid rotations. Part 2," *J. Fluid Mech.* **26**(1), 131–144 (1966).
- ²³I. Sumita and M. I. Bergman, "Inner-core dynamics," in *Treatise on Geophysics*, edited by P. Olson (Elsevier, 2007), Vol. 8, pp. 299–318.
- ²⁴J. B. Taylor, "The magneto-hydrodynamics of a rotating fluid and the Earth's dynamo problem," *Proc. R. Soc. London, Ser. A* **9**, 274–283 (1963).
- ²⁵J. Wicht and U. R. Christensen, "Torsional oscillations in dynamo simulations," *Geophys. J. Int.* **181**, 1367–1380, doi:10.1111/j.1365-246X.2010.04581.x (2010).